This article was downloaded by: [Renmin University of China]
On: 13 October 2013, At: 10:27
Publisher: Taylor & Francis
Informa Ltd Registered in England and Wales Registered Number: 1072954 Registered office: Mortimer House, 37-41 Mortimer Street, London W1T 3JH, UK

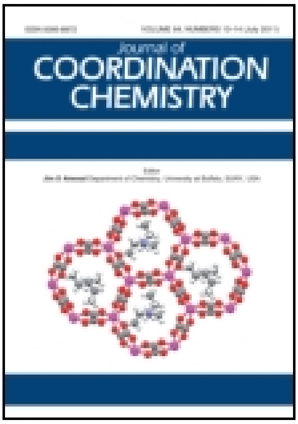

Journal of Coordination Chemistry
Publication details, including instructions for authors and subscription information:
http://www.tandfonline.com/loi/gcoo20

Two linear trinuclear clusters with bridging triazole: crystal structure and magnetism

Jie Yang [a] , Yun-Sheng Ma [a] , Xiao-Yan Tang [a] , Lei Shen [a] , Rong-Xin Yuan [a] & Dun-Ru Zhu [b]

[a] Department of Chemistry and Materials Engineering , Jiangsu Key Laboratory of Advanced Functional Materials, Changshu Institute of Technology , Changshu 215500, P.R. China

[b] College of Chemistry and Chemical Engineering, State Key Laboratory of Materials-oriented Chemical Engineering, Nanjing University of Technology , Nanjing 210009, P.R. China

Published online: 26 Sep 2011.

To cite this article: Jie Yang , Yun-Sheng Ma , Xiao-Yan Tang , Lei Shen , Rong-Xin Yuan & Dun-Ru Zhu (2011) Two linear trinuclear clusters with bridging triazole: crystal structure and magnetism, Journal of Coordination Chemistry, 64:19, 3291-3302, DOI: 10.1080/00958972.2011.616929

To link to this article: http://dx.doi.org/10.1080/00958972.2011.616929

PLEASE SCROLL DOWN FOR ARTICLE

Taylor & Francis makes every effort to ensure the accuracy of all the information (the "Content") contained in the publications on our platform. However, Taylor & Francis, our agents, and our licensors make no representations or warranties whatsoever as to the accuracy, completeness, or suitability for any purpose of the Content. Any opinions and views expressed in this publication are the opinions and views of the authors, and are not the views of or endorsed by Taylor & Francis. The accuracy of the Content should not be relied upon and should be independently verified with primary sources of information. Taylor and Francis shall not be liable for any losses, actions, claims, proceedings, demands, costs, expenses, damages, and other liabilities whatsoever or howsoever caused arising directly or indirectly in connection with, in relation to or arising out of the use of the Content.

This article may be used for research, teaching, and private study purposes. Any substantial or systematic reproduction, redistribution, reselling, loan, sub-licensing, systematic supply, or distribution in any form to anyone is expressly forbidden. Terms &

Journal of Coordination Chemistry
Vol. 64, No. 19, 10 October 2011, 3291–3302

Two linear trinuclear clusters with bridging triazole: crystal structure and magnetism

JIE YANG†, YUN-SHENG MA†, XIAO-YAN TANG†, LEI SHEN†,
RONG-XIN YUAN*† and DUN-RU ZHU‡

†Department of Chemistry and Materials Engineering, Jiangsu Key Laboratory of Advanced Functional Materials, Changshu Institute of Technology, Changshu 215500, P.R. China
‡College of Chemistry and Chemical Engineering, State Key Laboratory of Materials-oriented Chemical Engineering, Nanjing University of Technology, Nanjing 210009, P.R. China

(*Received 9 June 2011; in final form 4 August 2011*)

Two linear trinuclear clusters, $[Co_3(L)_6(H_2O)_6](ClO_4)_6$ (**1**) and $[Ni_3(L)_6(H_2O)_6](ClO_4)_6 \cdot 3H_2O$ (**2**) (L = 4-(4-hydroxyphenyl)-1,2,4-triazole), obtained by the reactions of $M(ClO_4)_2 \cdot 6H_2O$ and 4-(4-hydroxyphenyl)-1,2,4-triazole have been isolated and structurally characterized. The two isostructural clusters, linear hexapositive trimers, are linked by three N1,N2-1,2,4-triazoles to the divalent central and terminal metal ions. The magnetic behaviors of the clusters were investigated from 1.8 to 300 K. Magnetic susceptibility measurements reveal antiferromagnetic exchange interactions between the metal centers in the clusters. The magnetic data were analyzed by using linear trinuclear modes with $S = 3/2$ and $S = 1$ for **1** and **2**, respectively. Further studies were performed by accounting spin–orbital coupling for **1** and involving zero-field splitting within the ground state for **2**.

Keywords: Cluster; Trinuclear; Antiferromagnetic exchange interactions; Magnetochemistry; Cobalt; Nickel

1. Introduction

The syntheses and characterization of polynuclear clusters of paramagnetic metal ions have been of intense interest due to their intriguing structures and their potential applications in magnetochemistry and bioinorganic chemistry [1–9]. The discovery of single-molecule magnets (SMMs) has great significance since it suggests the possibility of employing molecules as the smallest possible particle for storage of magnetic information [1–3]. Spin crossover phenomena have also been observed in polynuclear compounds, with potential applications in information storage [10]. To achieve some kinds of magnetic coupling in magnetic metal-organic materials, the distance between the paramagnetic metal ions must be within the interacting range. Generally, short and conjugated ligands can transmit efficient magnetic coupling. 1,2,4-Triazole is

---

*Corresponding author. Email: yuanrx@hotmail.com

Journal of Coordination Chemistry
ISSN 0095-8972 print/ISSN 1029-0389 online
DOI: 10.1080/00958972.2011.616929

exo-bidentate toward metal ions, yielding polynuclear compounds whose nuclearity can be controlled by appropriate substituents on the azole ring, using suitable end-cap ligands or anions of different donor abilities [11–16]. As a bridging ligand, triazole offers a short two-atom pathway for magnetic exchange coupling. In addition, the chelating nitrogen donors can support the very strong ligand field in ferrous complexes to induce a transition from HS to LS state on cooling or increasing pressure [17].

Interesting magneto-structural correlation has also been observed with this ligand. By the analysis of magnetic and structural data for various dinuclear Cu(II) compounds, it became evident that singlet-triplet splitting varies with the variation of the Cu–N–N angle. The most symmetric N1,N2-1,2,4-triazole bridging mode, with all Cu–N–N angles close to 135° and with N–Cu–N innermost angles close to 90°, leads to the largest absolute value for $-2J$, on the order of $240\,\mathrm{cm}^{-1}$. A more asymmetric bridging mode will lead to a less efficient magnetic orbital overlap and the isotropic exchange constant decreases [18, 19].

To study more detailed magnetic–structural correlations for Co and Ni compounds, 4-(4-hydroxyphenyl)-1,2,4-triazole was used. In this article, we report preparative, structural, and magnetic studies of two linear trinuclear clusters $[Co_3(L)_6(H_2O)_6](ClO_4)_6$ (**1**) and $[Ni_3(L)_6(H_2O)_6](ClO_4)_6 \cdot 3H_2O$ (**2**) to understand the structure–magnetic property correlations.

2. Experimental

2.1. *General*

All starting materials were of reagent grade and used as purchased from Aldrich. The ligand (L) was synthesized according to the literature method [20]. Elemental analyses were performed on a PE 240 elemental analyzer. FT-IR spectra were recorded on a NICOLET 380 spectrometer using pressed KBr pellets. Variable temperature magnetic susceptibilities of crystalline samples were measured on a Quantum Design MPMS SQUID-XL7 magnetometer. The magnetic data were corrected for diamagnetic contributions of both the sample holder and the compound obtained from Pascal's constants [21].

Single crystal X-ray data were collected on a Rigaku SCX mini CCD diffractometer equipped with graphite-monochromated Mo-Kα radiation ($\lambda = 0.071073$ Å). Intensity data were collected by the ω scan technique and reduced using the Crystal-Clear program [22]. The structures were solved by direct methods using SHELXTL [23] and refined by full-matrix least-squares on F^2. All non-hydrogen atoms were refined anisotropically and hydrogen atoms were included in the final stage of the refinement on calculated positions bonded to their carrier atoms. The phenyl, hydroxyl, and perchlorates in **1** and **2** were found to be disordered over two sites with an occupancy ratio of 0.5974/0.4026 (**1**) or 0.0.6577/0.3423 (**2**) for (C(1)–C(6))/(C(1A)–C(6A)), O(1)/O(1A), and (Cl(1)–O(4))/(Cl(1A)–O(4A)). The hydrogen atoms of water were located from Fourier maps. All other hydrogen atoms were placed in geometrically idealized positions (C–H = 0.95 Å for phenyl) and constrained to ride on their parent atoms with $U_{iso}(H) = 1.2U_{eq}(C)$ for phenyl groups. Crystallographic data and selected bond lengths and angles are listed in tables 1 and 2.

Table 1. Crystallographic data for **1** and **2**.

Complex	**1**	**2**
Molecular formula	$C_{48}H_{54}Cl_6Co_3N_{18}O_{36}$	$C_{48}H_{60}Cl_6N_{18}Ni_3O_{39}$
Formula weight	1848.58	1901.91
Size (mm^3)	0.20 × 0.18 × 0.12	0.38 × 0.26 × 0.20
Crystal color	Yellow	Purple
Crystal system	Trigonal	Trigonal
Space group	*R*-3	*R*-3
Unit cell dimensions (Å, 0)		
a	16.449(17)	16.375(17)
b	16.449(17)	16.375(17)
c	26.413(5)	26.152 (5)
Volume (Å^3), *Z*	6189.1(15), 3	6072.9(15), 3
Calculated density (g cm^{-3})	1.488	1.560
Temperature (K)	223(2)	223(2)
Absorption coefficient (Mo-Kα) (mm^{-1})	0.883	0.987
θ range (°)	3.9–24.9	3.3–25.0
Total reflections	16,512	11,027
Unique reflections	2128 ($R_{\text{int}} = 0.112$)	2244 ($R_{\text{int}} = 0.032$)
Data/parameters	9068/241	5122/244
R^a	0.1257	0.0684
wR^b	0.2578	0.1898
Goodness-of-fit on $F^{2\ c}$	1.011	1.085
Largest difference peak and hole (e Å^{-3})	1.702 and −0.434	1.164 and −0.642

$^a R = \Sigma||F_o| - |F_c||/\Sigma|F_o|$; $^b wR = \{\Sigma w(F_o^2 - F_c^2)^2/\Sigma w(F_o^2)^2\}^{1/2}$; ^{c}Goodness-of-fit $= \{\Sigma[w((F_o^2 - F_c^2)^2)](n - p)\}^{1/2}$.
Where n = number of reflections and p = total numbers of parameters refined.

Table 2. Selected bond lengths (Å) and angles (°) for **1** and **2**.

Co(1)–N(2)	2.147(6)	Ni(1)–N(2)	2.108(3)
Co(2)–N(1)	2.100(6)	Ni(2)–N(1)	2.042(3)
Co(2)–O(2)	2.101(6)	Ni(2)–O(2)	2.072(3)
N(2)–Co(1)–N(2)C	91.1(2)	N(2)–Ni(1)–N(2)C	89.37(13)
N(1)–Co(2)–O(2)	90.8(3)	N(1)–Ni(2)–O(2)C	89.16(14)
N(1)–Co(2)–N(1)A	89.7(3)	N(1)–Ni(2)–N(1)C	91.33(14)
N(1)–Co(2)–O(2)A	89.9(2)	N(1)–Ni(2)–O(2)B	90.32(15)
N(1)–Co(2)–O(2)D	179.3(2)	N(1)–Ni(2)–O(2)	178.26(14)
O(2)–Co(2)–O(2)A	89.6(2)	O(2)–Ni(2)–O(2)B	89.17(15)

Symmetry codes: A $-y+2, x-y+1, z$; B $y, -x+y+1, -z+1$; C $x-y+1, x, -z+1$; D $-x+y+1, -x+2, z$ for **1** and A $-x+4/3, -y+2/3, -z+5/3$; B $-y+1, x-y, z$; C $-x+y+1, -x+1, z$; D $y+1/3, -x+y+2/3, -z+5/3$ for **2**.

2.2. *Syntheses of the cluster compounds*

2.2.1. Synthesis of $[Co_3(L)_6(H_2O)_6](ClO_4)_6$ (1). A mixture of $Co(ClO_4)_2 \cdot 6H_2O$ (36.59 mg, 0.1 mmol) and 4-(4-hydroxyphenyl)-1,2,4-triazole (32.03 mg, 0.2 mmol) in EtOH (5 mL) were sealed in a 25 mL Telfon-lined stainless steel container and heated at 120°C for 72 h. After the sample was cooled to room temperature at a rate of 5°C h^{-1}, yellow block crystals were obtained in *ca* 53% yield based on Co. Anal. Calcd for $C_{48}H_{54}Cl_6Co_3N_{18}O_{36}$ (%): C, 31.19; H, 2.94; N, 13.64. Found: C, 31.49; H, 3.21; N, 13.31. FT-IR (KBr, cm^{-11}): 3421(br), 1613(m), 1549(vs), 1514(vs), 1115(s), 1079(s), 626(s).

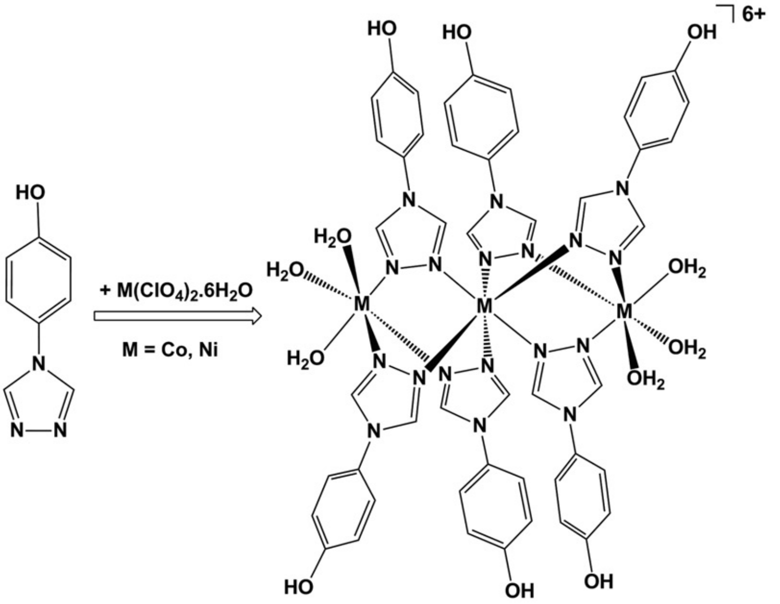

Scheme 1. Reactions of 4-(hydroxyphenyl)-1,2,4-triazole with $Co(ClO_4)_2 \cdot 6H_2O$ and $Ni(ClO_4)_2 \cdot 6H_2O$.

2.2.2. Synthesis of $[Ni_3(L)_6(H_2O)_6](ClO_4)_6 \cdot 3H_2O$ (2). Compound **2** was prepared by a similar experimental procedure except that $Ni(ClO_4)_2 \cdot 6H_2O$ was used. Purple crystals were obtained in *ca* 55% yield based on Ni. Anal. Calcd for $C_{48}H_{60}Cl_6N_{18}Ni_3O_{39}$ (%): C, 30.31; H, 3.18; N, 13.26. Found: C, 30.03; H, 3.24; N, 12.98. FT-IR (KBr, cm^{-1}): 3434(br), 1611(m), 1549(vs), 1514(vs), 1116(s), 1080(s), 628(s).

3. Results and discussion

3.1. *Syntheses and spectroscopic properties of the complexes*

Compounds **1** and **2** were obtained through solvo-thermal reactions of $Co(ClO_4)_2 \cdot 6H_2O$ or $Ni(ClO_4)_2 \cdot 6H_2O$ and 4-(4-hydroxyphenyl)-1,2,4-triazole in EtOH at 120°C (scheme 1). When the reaction temperature is decreased to 85°C, an unknown pale precipitate was formed which was not characterized. The molar ratio of the starting materials is also important in the formation of pure product. Increase in the amount of 4-(4-hydroxyphenyl)-1,2,4-triazole [$L : M(ClO_4)_2 \cdot 6H_2O = 1 : 1$] favors the precipitation of the ligand, while reduction in the amount of 4-(4-hydroxyphenyl)-1,2,4-triazole [$L : M(ClO_4)_2 \cdot 6H_2O = 1 : 2$] favors the formation of the uncharacterized pale precipitate.

IR spectra of **1** and **2** showed strong and broad stretching bands centered at 3421 cm^{-1} and 3434 cm^{-1}, respectively, which are attributed to O–H stretching vibration for free or bonded water. The free 4-(4-hydroxyphenyl)-1,2,4-triazole spectrum shows two strong bands at 1531 and 1483 cm^{-1}, attributable to vibrations

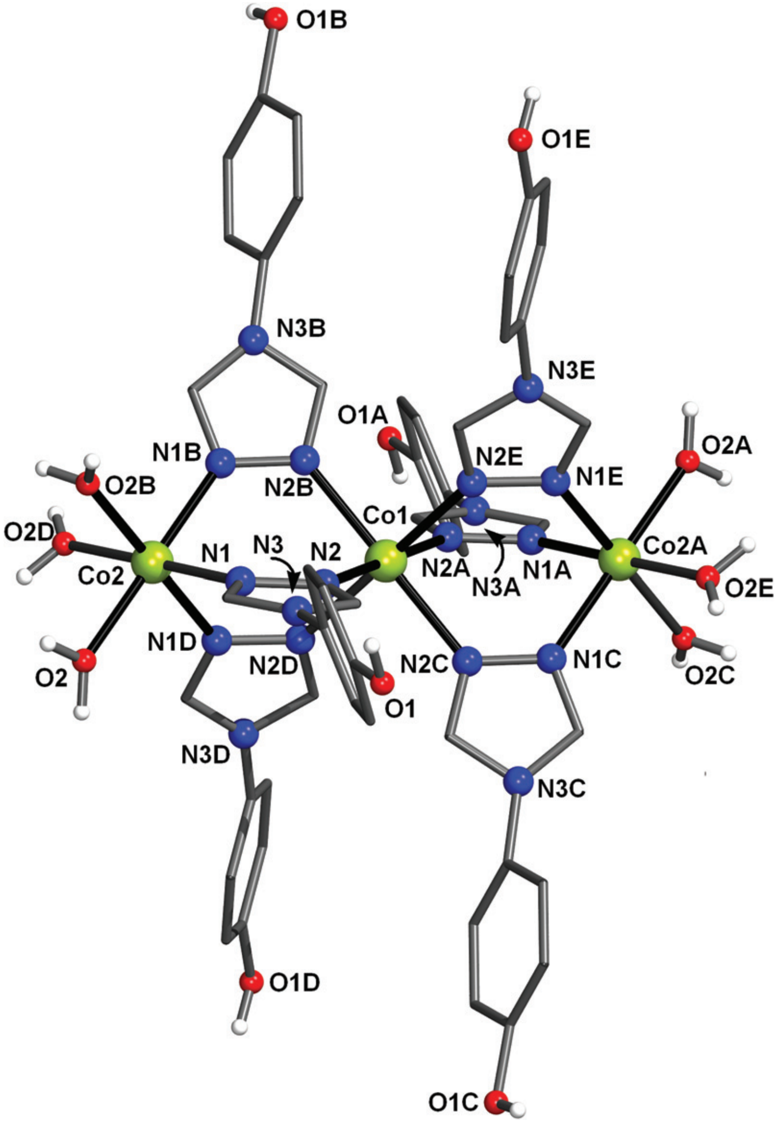

Figure 1. Perspective view of trinuclear cation of **1**. All hydrogen atoms (except from hydroxyl and water) have been omitted for clarity.

of the triazole ring. Upon triazole coordination to Co(II) the bands are red-shifted by +18 and +31 wavenumbers to 1549 and 1514 cm^{-1}. The strong bands for **1** and **2** centered at 1115, 1079, and 626 cm^{-1} were assigned to ClO_4^- [24].

3.2. *Description of crystal structures*

The core structures of **1** and **2** have similar structural features (figures 1 and 2). Both clusters consist of linear trinuclear cations with a +6 charge, and non-coordinated

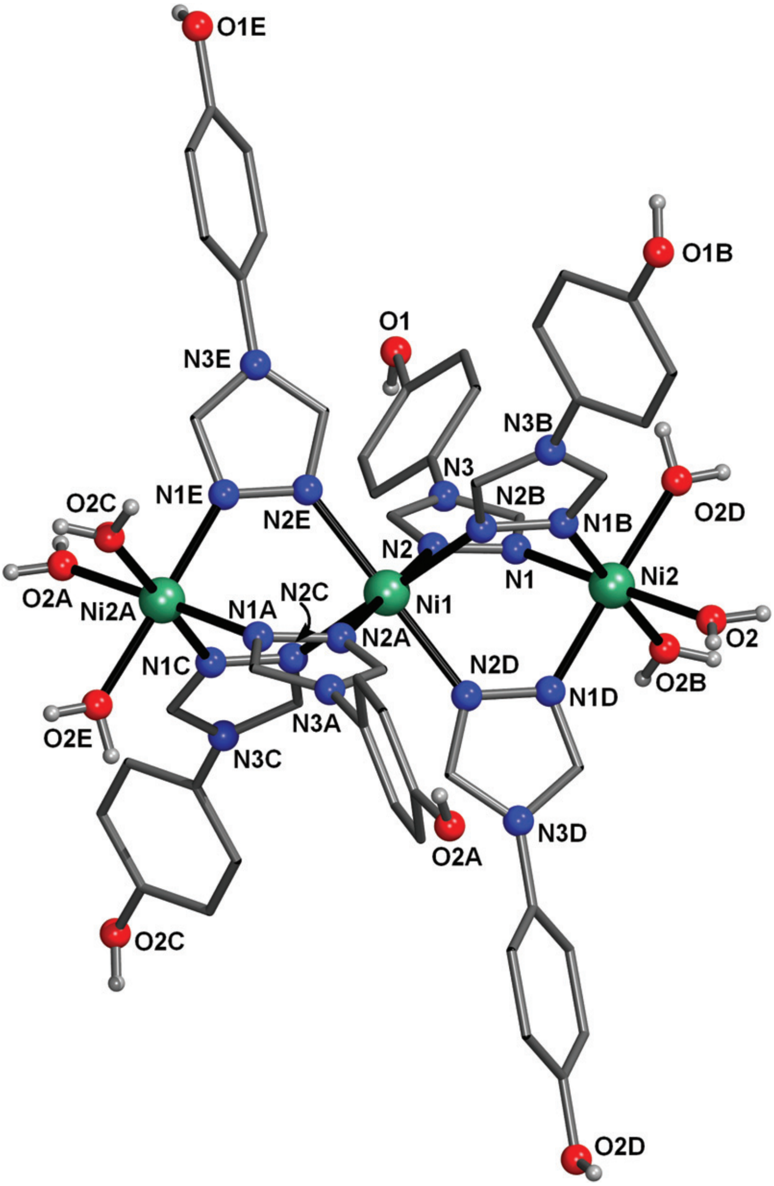

Figure 2. Perspective view of trinuclear cation of **2**. All hydrogen atoms (except from hydroxyl and water) have been omitted for clarity.

perchlorates and solvent. The central M^{n+} lies on the inversion center and is triply bridged to each external M^{n+} by the ligands through nitrogen atoms in the 1,2-positions. Each external M^{n+} completes its octahedron with three water molecules. The center metals in both cases are surrounded by six nitrogen atoms to form almost perfect MN_6 octahedra with bond angles very close to 90° [88.9(2)–91.1(2)° for **1** and 89.37(14)–90.63(14)° for **2**]. The M–N distances are in the normal ranges and averaged about 0.05–0.07 Å longer than the terminal ones [M–N$_{\text{center}} = 2.147$ Å for **1** and 2.108 Å for **2**; M–N$_{\text{terminal}} = 2.100(6)$ Å for **1** and 2.042(3) Å for **2**]. This difference in bond-lengths is attributed to steric hindrance [14]. The nearest M$\cdots$M distances are 3.866(2) Å for **1** and 3.765(1) Å for **2**. The M–N–N angles are 124.90° for **1** and 124.59° for **2**.

3.3. *Magnetic properties*

Complexes **1** and **2** were studied by magnetic susceptibility measurements from 1.8 to 300 K. For a linear trinuclear compound, the magnetic susceptibility is calculated using the Hamiltonian $\hat{H} = -2J[\hat{S}_1 \cdot \hat{S}_2 + \hat{S}_2 \cdot \hat{S}_3]$, assuming that the exchange integrals between the neighboring metal are identical ($J_{12} = J_{23} = J$) and the integral between the terminal metal ions is zero ($J_{13} = 0$) [21]. The molar magnetic susceptibility for such a trinuclear complex is given in equation (1), where $\chi_{\text{trinuclear}}$ denotes the susceptibility per trinuclear complex and the other symbols have their usual meanings.

$$\chi_{\text{trinuclear}} = \frac{Ng^2\beta^2}{4kT} \times \frac{A}{B}. \tag{1}$$

For **1** ($S = 3/2$):

$$\begin{aligned} A &= 94 + 10\mathrm{e}^{-12J/kT} + \mathrm{e}^{-9J/kT} + 35\mathrm{e}^{-7J/kT} + 10\mathrm{e}^{-6J/kT} + \mathrm{e}^{-5J/kT} + 10\mathrm{e}^{-2J/kT} \\ &\quad + 35\mathrm{e}^{-J/kT} + 35\mathrm{e}^{3J/kT} + 84\mathrm{e}^{6J/kT} + 165\mathrm{e}^{9J/kT}. \\ B &= 6 + 2\mathrm{e}^{-12J/kT} + \mathrm{e}^{-9J/kT} + 3\mathrm{e}^{-7J/kT} + 2\mathrm{e}^{-6J/kT} + \mathrm{e}^{-5J/kT} + 2\mathrm{e}^{-2J/kT} + 3\mathrm{e}^{-J/kT} \\ &\quad + 3\mathrm{e}^{3J/kT} + 4\mathrm{e}^{6J/kT} + 5\mathrm{e}^{9J/kT}. \end{aligned}$$

For **2** ($S = 1$):

$$\begin{aligned} A &= 48 + 8\mathrm{e}^{-4J/kT} + 8\mathrm{e}^{2J/kT} + 40\mathrm{e}^{4J/kT} + 112\mathrm{e}^{6J/kT}. \\ B &= 8 + 3\mathrm{e}^{-4J/kT} + \mathrm{e}^{-2J/kT} + 3\mathrm{e}^{2J/kT} + 5\mathrm{e}^{4J/kT} + 7\mathrm{e}^{6J/kT}. \end{aligned}$$

When the intercluster interaction is taken into account, the expression for χ_{M} is:

$$\chi_{\mathrm{M}} = \frac{\chi_{\text{trinuclear}}}{1 - (2zj'/Ng^2\beta^2)\chi_{\text{trinuclear}}}. \tag{2}$$

The magnetic behavior of **1** is shown in figure 3 in the form of χ_{M}, $\chi_{\mathrm{M}}T$ *versus* T plots. The $\chi_{\mathrm{M}}T$ value at 300 K is 8.01 cm^3 K mol^{-1}, larger than the expected value of 5.63 cm^3 K mol^{-1} for three magnetically isolated high spin Co(II) ($S = 3/2$) ions with $g = 2$, indicating that an important orbital contribution is involved in the complex due to the distorted octahedral geometry of the Co(II) [25, 26]. As T is lowered, $\chi_{\mathrm{M}}T$ decreases more and more rapidly and reaches 1.71 cm^3 K mol^{-1} at 1.8 K. Considering the presence of spin–obit coupling due to the $^4\mathrm{T}_{1\mathrm{g}}$ ground state for octahedral Co(II), exact calculations for deriving J from experimental data in all the temperature ranges is nearly impossible [27]. The susceptibility data for **1** was fitted using equation (1) in the temperature range of 10–300 K with the best fit parameters, $g = 2.57$, $J = -4.83$ cm^{-1}, $zJ' = -1.65$ cm^{-1}. The agreement factor $R = [\sum|(\chi_{\mathrm{M}})_{\mathrm{obs}} - (\chi_{\mathrm{M}})_{\mathrm{calc}}|^2 / \sum(\chi_{\mathrm{M}})^2_{\mathrm{obs}}]$ is 5.8×10^{-4}. The negative J suggests antiferromagnetic exchange between metal centers

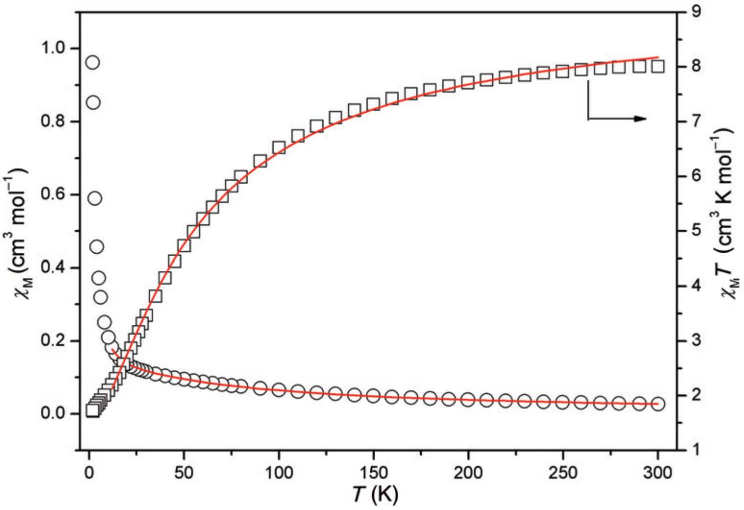

Figure 3. Plots of χ_M, $\chi_M T$ *vs.* T for **1** fitted by using the trinuclear model. The solid lines denote the theoretical fit of the experimental data.

in **1**. The antiferromagnetic exchange is weaker than that in the triple triazole-bridged trimer $[Co(t\text{-}Butrz)_8(CNS)_2] \cdot 2CNS \cdot 9H_2O$ ($J = -9.0\,cm^{-1}$) [28].

The fit does not work well in the whole temperature range as it does not account for spin–orbital coupling. To get a reasonable estimate of the strength of the antiferromagnetic exchange interaction as well as the spin–orbital coupling, a simple equation was introduced by Rueff [29, 30] as shown below.

$$\chi_M = \frac{A\exp(-E_1/kT) + B\exp(-E_2/kT)}{T}, \tag{3}$$

where A + B equals the Curie constant and E_1, E_2 represent the 'activation energies' corresponding to the spin–orbital coupling and the antiferromagnetic exchange interaction, respectively. The fitting of the experimental data using this model gives $A + B = 9.1\,cm^3\,K\,mol^{-1}$, $-E_1/k = -48.1\,K$, $-E_2/k = -0.4\,K$, $R = 2.6 \times 10^{-4}$ (figure 4). The $-E_2/k$ value found for the antiferromagnetic exchange interaction is weak and corresponds to $J = -0.8\,K$ ($-0.56\,cm^{-1}$).

The magnetic behavior of **2** is shown in figure 5 in the form of χ_M, $\chi_M T$ *versus* T plots. The value of $\chi_M T$ at 300 K is $3.26\,cm^3\,K\,mol^{-1}$, which is close to the expected value of $3.00\,cm^3\,K\,mol^{-1}$ for three magnetically isolated high-spin Ni(II) ions. As T is lowered, $\chi_M T$ decreases gradually to $1.22\,cm^3\,K\,mol^{-1}$ at 1.8 K. This behavior is due to the presence of a dominant antiferromagnetic interaction between adjacent Ni(II) ions. The best fit of the theoretical equation (1) to experimental data in whole temperature range leads to $g = 2.18$, $J = -9.35\,cm^{-1}$, $zJ' = 0.06\,cm^{-1}$ with an agreement factor $R = 1.5 \times 10^{-4}$. The negative J suggests antiferromagnetic exchange interactions between Ni(II) in **2**. The zJ' is much smaller than the J value, indicating weak exchange interaction between adjacent trinuclear molecules. The magnetic properties of **2** are quite similar to that of antiferromagnetic $[Ni_3(guanazole)_6(NCS)_6] \cdot 6H_2O$ ($J = -10.32\,cm^{-1}$, guanazole = 3,5-diamino1,2,4-triazole) [31] and $[Ni_3(L)_6(H_2O)_6]Cl_6 \cdot 10H_2O$ ($J = -7.9\,cm^{-1}$, L = 3,5-dimethanyl-4amino-1,2,4-triazole) [15]. The results

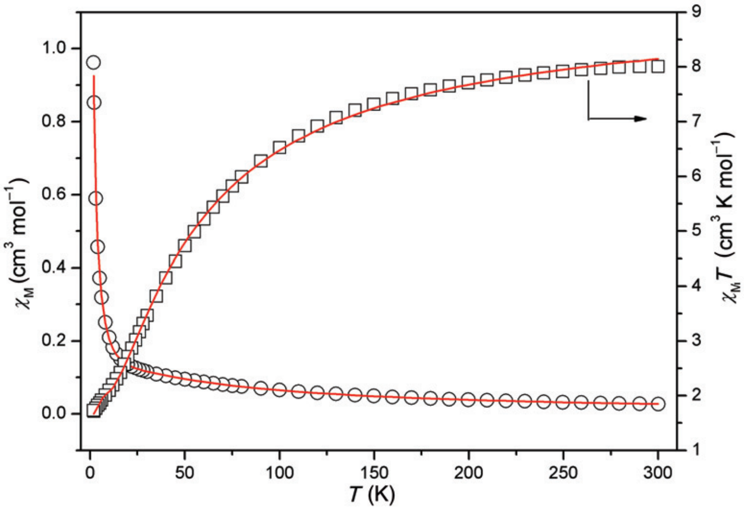

Figure 4. Plots of χ_M, $\chi_M T$ *vs.* T for **1** fitted using equation (3). The solid lines denote the theoretical fit of the experimental data.

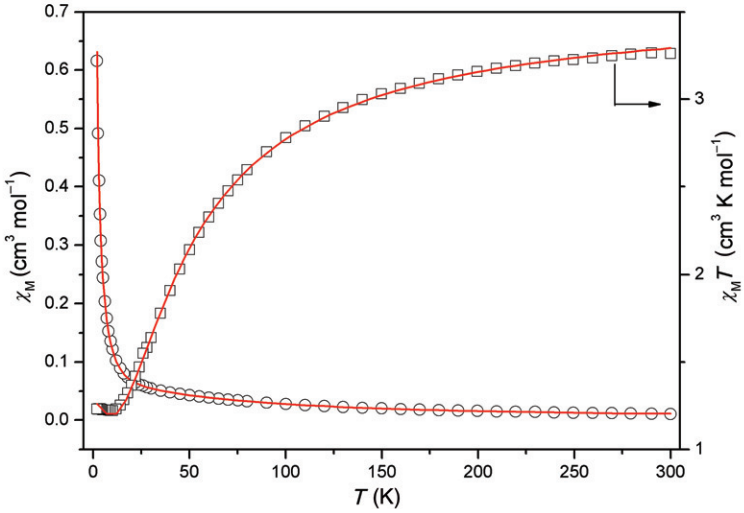

Figure 5. Plots of χ_M, $\chi_M T$ *vs.* T for **2** fitted using the trinuclear model. The solid lines denote the theoretical fit of the experimental data.

indicate that different substituents in the triazole ligands do not noticeably affect the efficiency of the antiferromagnetic exchange interactions in these clusters.

The magnetic analysis was further carried out using the spin Hamiltonian $\hat{H}=-2J(\hat{S}_1\hat{S}_2+\hat{S}_2\hat{S}_3)+D[\hat{S}_z{}^2-\mathrm{S}(\mathrm{S}+1)/3]\delta_{\mathrm{S,S}=3}$ involving zero-field splitting within the ground state by D parameters, so the resulting magnetic

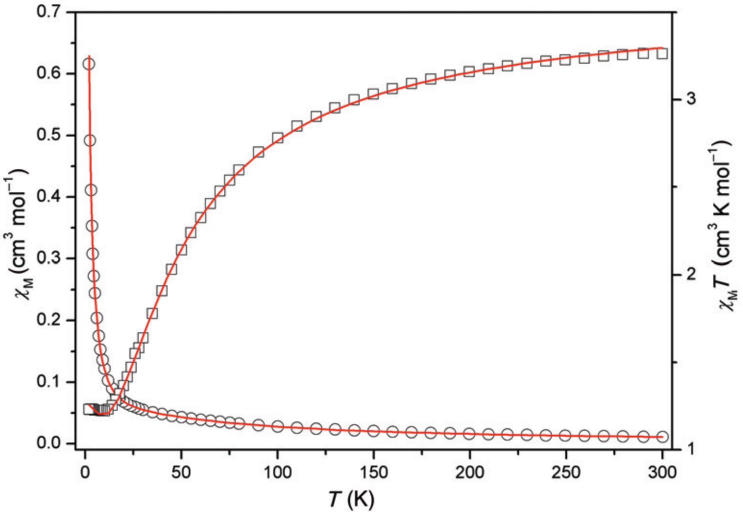

Figure 6. Plots of χ_M, $\chi_M T$ *vs.* T for **2** fitted using equation (4). The solid lines denote the theoretical fit of the experimental data.

susceptibility equation is:

$$\chi_M = \frac{Ng^2\beta^2}{kT}\left(\frac{A}{B}\right). \tag{4}$$

$$A = 18e^{-5D/kT} + 2e^{3D/kT} + 8 + 10e^{-6J/kT} + 2e^{-10J/kT} + 10e^{-2J/kT} + 2e^{-6J/kT} + 2e^{-4J/kT},$$
$$B = 2e^{-5D/kT} + 2e^{-3D/kT} + e^{4D/kT} + 2 + 5e^{-6J/kT} + 3e^{-10J/kT} + 5e^{-2J/kT} + 3e^{-6J/kT} + e^{-8J/kT} + 3e^{-4J/kT},$$

where J is the intramolecular exchange integral between nickel(II) ions, D is the zero-field splitting parameter, and the other symbols have their usual meanings [32]. The best fitting for the experimental data gives $g = 2.19$, $J = -9.24\,\text{cm}^{-1}$, $D = 0.73\,\text{cm}^{-1}$, $R = 1.9 \times 10^{-4}$ (figure 6). Introduction of a zero-field splitting term did not change the fitting significantly, and an estimate of $D = 0.73\,\text{cm}^{-1}$ was obtained with very slight change in J, indicating that the dominant effect is weak intramolecular antiferromagnetic exchange.

4. Conclusion

We compare and contrast the syntheses, structures, and magnetic properties of two linear trinuclear clusters of general formula $[M_3(L)_6(H_2O)_6](ClO_4)_6 \cdot H_2O$. A weak antiferromagnetic interaction is found in the linear trinuclear triply N1,N2-1,2,4-triazole-bridged compounds. The structure is different from $[Ni_3O(H_2L)(L)_2] \cdot 2DMF$ that has a triangle structure [33]. The magnetic interaction is weaker than that in $\{[Ni_3(dpa)_4(1,4\text{-bdc})] \cdot 0.5H_2O\}_n$ with 2,2′-dipyridylamido anion as bridge, although the structures are similar [34]. The exchange parameters lie in the range observed for 4-substituted triazoles, which might be expected from the similarity of the overall structures of the compounds. Further research is in progress to produce other clusters based on triazoles; future directions might include attaching clusters on the surface of colloids with suitable complementary charge as shown with other metal clusters and to observe the magnetic behaviors thereof [35–37].

Supplementary material

CCDC 753450 and 753451 contain the supplementary crystallographic data for **1** and **2**. Crystallographic data for the structural analyses have been deposited with the Cambridge Crystallographic Data Center. Copies of this information can be had free of charge from CCDC, 12 Union Road, Cambridge CB2 1EZ, UK (Fax: +44-1223-336-033; E-mail: deposit@ccdc.ac.uk).

Acknowledgments

This work was supported by the Natural Science Fund of Jiangsu Province of P.R. China (No. 08KJB150001), NSFC (Nos 20971017, 21001018), and the start-up grant from CSLG (No. KYZ2010131Z).

References

[1] G. Christou. *Acc. Chem. Res.*, **22**, 328 (1989).
[2] S. Hill, R.S. Edwards, N. Aliaga-Alcalde, G. Christou. *Science*, **302**, 1015 (2003).
[3] R. Bagai, G. Christou. *Chem. Soc. Rev.*, **38**, 1011 (2009).
[4] D. Gatteschi, R. Sessoli. *Angew. Chem. Int. Ed.*, **42**, 268 (2003).
[5] G. Aromi, E.K. Brechin. *Struct. Bond.*, **122**, 1 (2006).
[6] E.K. Brechin. *Chem. Commun.*, 5141 (2005).
[7] J. Klingele, S. Dechert, F. Mayer. *Coord. Chem. Rev.*, **253**, 2698 (2009).
[8] M. Atanasov, P. Comba, S. Hausberg, B. Martin. *Coord. Chem. Rev.*, **253**, 2306 (2009).
[9] S. Groysman, R.H. Holm. *Biochemistry*, **48**, 2310 (2009).
[10] J. Kröber, E. Codjovi, O. Kahn, F. Grolière, C. Jay. *J. Am. Chem. Soc.*, **115**, 9810 (1993).
[11] P.J. van Koningsbruggen, D. Gatteschi, R.A.G. de Graaff, J.G. Haasnoot, J. Reedijk, C. Zanchini. *Inorg. Chem.*, **34**, 5175 (1995).
[12] J.G. Haasnoot. *Coord. Chem. Rev.*, **200**, 131 (2000).
[13] J.-H. Zhou, R.-M. Cheng, Y. Song, Y.-Z. Li, Z. Yu, X.-T. Chen, Z.-L. Xue, X.-Z. You. *Inorg. Chem.*, **44**, 8011 (2005).
[14] B. Liu, L. Xu, G.-C. Guo, J.-S. Huang. *J. Mol. Struct.*, **825**, 79 (2006).
[15] Q.-G. Zhai, X.-Y. Wu, S.-M. Chen, C.-Z. Lu, W.-B. Yang. *Cryst. Growth Des.*, **6**, 2126 (2006).
[16] B. Ding, L. Yi, W.-Z. Shen, P. Cheng, D.-Z. Liao, S.-P. Yan, Z.-H. Jiang. *J. Mol. Struct.*, **784**, 138 (2006).
[17] M. Thomann, O. Kahn, J. Guilhem, F. Varret. *Inorg. Chem.*, **33**, 6029 (1994).
[18] P.M. Slangen, P.J. van Koningsbruggen, K. Goubitz, J.G. Haasnoot, J. Reedijk. *Inorg. Chem.*, **33**, 1121 (1994).
[19] P.M. Slangen, P.J. van Koningsbruggen, J.G. Haasnoot, J. Jansen, S. Gorter, J. Reedijk, H. Kooijman, W.J.J. Smeets, A.L. Spek. *Inorg. Chim. Acta*, **212**, 289 (1993).
[20] R.H. Wiley, A.J. Hart. *J. Org. Chem.*, **18**, 1368 (1953).

[21] O. Kahn. *Molecular Magnetism*, VCH Publishers, New York (1993).
[22] *Rigaku CrystalClear*, Rigaku Corporation, Tokyo, Japan (2005).
[23] G.M. Sheldrick. *Acta Cryst.*, **A64**, 112 (2008).
[24] K. Nakamoto. *Infrared and Raman Spectra of Inorganic and Coordination Compounds, Part B*, p. 86, Wiley & Sons, New York (2009).
[25] A. Rodriguez-Dieguez, J. Cano, R. Kivekas, A. Debdoubi, E. Colacio. *Inorg. Chem.*, **46**, 2503 (2007).
[26] S.R. Marshall, C.D. Incarvito, J.L. Manson, A.L. Rheingold, J.S. Miller. *Inorg. Chem.*, **39**, 1969 (2000).
[27] D. Ghoshal, G. Mostafa, T.K. Maji, E. Zangrando, T.H. Lu, J. Ribas, N.R. Chaudhuri. *New J. Chem.*, **28**, 1204 (2004).
[28] L.R. Groeneveld, R.A. le Fêbre, R.A.G. de Graaff, J.G. Haasnoot, G. Vos, J. Reedijk. *Inorg. Chim. Acta*, **102**, 69 (1985).
[29] J.M. Rueff, N. Masciocchi, P. Rabu, A. Sironi, A. Skoulios. *Eur. J. Inorg. Chem.*, 2843 (2001).
[30] J.M. Rueff, N. Masciocchi, P. Rabu, A. Sironi, A. Skoulios. *Chem. Eur. J.*, **8**, 1813 (2002).
[31] L. Antolini, A.C. Fabretti, D. Gatteschi, A. Giusti, R. Sessoli. *Inorg. Chem.*, **29**, 143 (1990).
[32] Q.-L. Wang, C. Yang, L. Qi, D.-Z. Liao, G.-M. Yang, H.-X. Ren. *J. Mol. Struct.*, **892**, 88 (2008).
[33] X.-Q. Shen, Z.-F. Li, H.-Y. Zhang, Z.-J. Li. *J. Coord. Chem.*, **63**, 1720 (2010).
[34] J. Zhang, Y. Deng, L.-G. Zhu. *J. Coord. Chem.*, **64**, 1654 (2011).
[35] S. Roy, M.C.D. Mourad, M.T. Rijneveld-Ockers. *Langmuir*, **23**, 399 (2007).
[36] S. Roy, H.J.D. Meeldijk, A.V. Petukhov, M. Versluijs, F. Soulimani. *Dalton Trans.*, 2861 (2008).
[37] S. Roy, L.C.A.M. Bossers, H.J.D. Meeldijk, B.W.M. Kuipers, W.K. Kegel. *Langmuir*, **24**, 666 (2008).